

Shaking table model tests on geogrid reinforced soil retaining wall with embedded sheetpile

Nakajima, S.

University of Tokyo, Japan

Koseki, J.

Institute of Industrial Science, University of Tokyo, Japan

Watanabe, K. & Tateyama, M.

Railway Technical Research Institute, Japan

Kato, N.

Japan Patent Office, Japan

Keywords: shaking table, model test, reinforced soil retaining walls, sheetpile, residual displacements

ABSTRACT: Based on the results from 1g shaking table model tests on retaining walls with embedded sheetpile, analysis on the effect of the sheetpile is carried out. It is also attempted to introduce the effect of the sheetpile into the formerly developed procedures to predict the earthquake-induced displacements of geogrid reinforced soil retaining walls. It is assumed that certain amount of shear force acting on the subsoil below the wall, which causes the wall displacement, is reduced by the existence of the sheetpile. The wall displacements calculated by the modified procedures are in good agreement with the measured ones.

1 INTRODUCTION

In the 1995 Hyogoken Nanbu-earthquake, geogrid reinforced soil retaining walls with full height rigid facing showed higher seismic performance than conventional concrete retaining walls like gravity and leaning type retaining walls. However, even in the former type retaining walls, certain amounts of residual displacements were observed. Especially in the urban area, it is required to reduce such residual displacements of the retaining walls to avoid the negative effect to the neighbouring structures and lifelines.

To reduce such residual displacements, aseismic countermeasure by embedding sheetpile was studied. Shaking table model tests were performed to evaluate the effect of the sheetpile, and a formerly developed procedure to predict residual displacements of the reinforced soil retaining wall was modified to consider the effect of the sheetpile based on the analysis of model test results.

2 MODEL TESTS

2.1 Procedures

In the model tests, as shown in Fig. 1, a full-height rigid facing model having a height of 500 mm was placed on subsoil layers consisting of dense dry Toyoura sand at a void ratio of about 0.639 (D_r is about 90%) which were prepared by air pluviation using a sand hopper. Backfill layers were also prepared

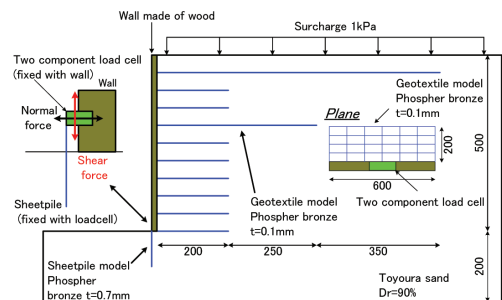


Figure 1. Cross-section of reinforced soil retaining wall with embedded sheetpile (unit in mm).

by Toyoura sand in the same manner as the subsoil layers. As a reinforcement model, grids of phosphor bronze strips having a thickness of 0.1 mm and a width of 3 mm, with sand particles glued on the surface of the strips, were placed in the backfill at a vertical spacing of 50 mm. Sheetpile model having an embedded depth of 10 cm, which was made by phosphor bronze plate having a thickness of 0.7 mm, was fixed with the wall facing at its toe.

These models were subjected to horizontal shaking with the irregular waves as shown in Fig. 2, where the maximum acceleration was increased gradually at an increment of about 100 gals.

2.2 Test results

Residual displacements of the model reinforced soil retaining wall with embedded sheetpile (RRWSP) in

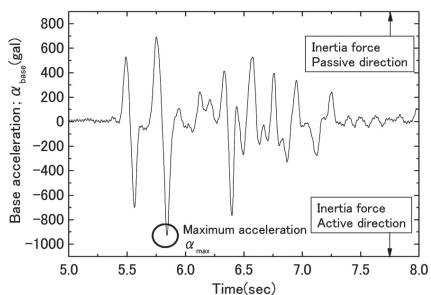


Figure 2. Typical time history of base acceleration.

terms of tilting angle and base sliding are plotted versus the amplitude of base acceleration in Fig. 3, where the result of normal reinforced retaining wall (RRW), which was formerly conducted, is also plotted. RRWSP showed higher seismic performance than RRW, especially in terms of tilting displacements.

Failure plane in the backfill of RRWSP developed from the bottom part to the surface of the backfill layer as shown in Photo 1. Residual displacements of RRWSP were increased rapidly after the full formation of the failure plane which was indicated by vertical arrows shown in Fig. 3. The same tendency was also observed in case of RRW.

3 MODELING

3.1 Formerly developed procedure

Koseki et al (2004) proposed a simplified procedure to evaluate residual displacements of the reinforced soil retaining wall. Sliding and overturning displacement of the wall facing due to accumulation of residual shear deformations of subsoil and reinforced backfill were computed, respectively.

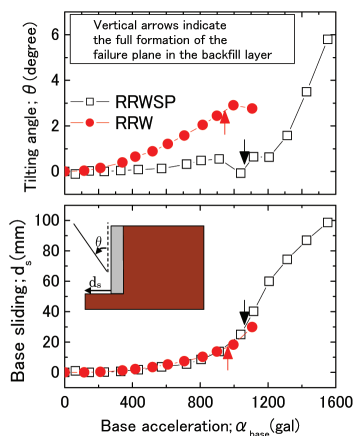


Figure 3. Relationships between residual displacements of wall facing base acceleration.

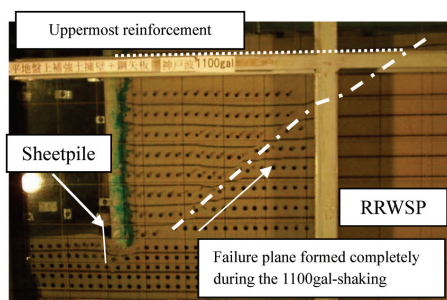


Photo 1. Formation of failure plane in backfill layers.

Formation of the failure plane in unreinforced backfill was also considered by computing the shear strain in the unreinforced backfill from the calculated sliding and overturning displacements. After its formation, in addition to the shear deformation of the subsoil and reinforced backfill, Newmark's sliding block method was also applied to compute the sliding component.

In this study, the above procedure was modified to take into account the effect of the sheetpile by assuming that the sheetpile would share some amount of the shear stress which would induce the shear deformation of the subsoil and reinforced backfill.

3.2 Shear deformation of subsoil layers with embedded sheetpile

In the formerly developed procedures, subsoil layers below the reinforced backfill were assumed as one macro element. To introduce the effect of sheetpile, as schematically shown in Fig. 4, subsoil layers were divided into two layers, one is the embedded layer, and the other is a layer below the embedded layer that will be referred as "sub layer" herein.

Relationships between the shear stress ratio $SR = \tau/\sigma$ and the shear strain that were mobilized in the embedded layer are shown in Fig. 5. Shear strain in the embedded layer was evaluated from the measured shear deformation of embedded layer, which was computed by the integration of the measured bending moment induced in the sheetpile, which was measured by the strain gages pasted on the surface of the

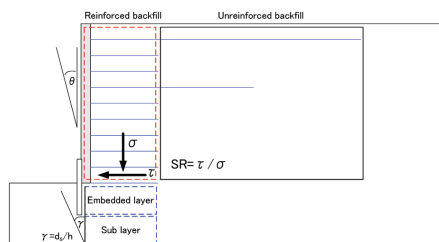


Figure 4. Schematic diagram of each subsoil layer and backfill.

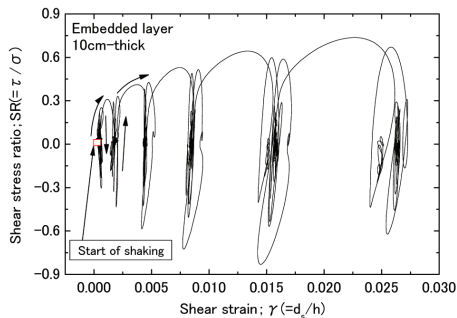


Figure 5. Stress-strain relationship of embedded layer.

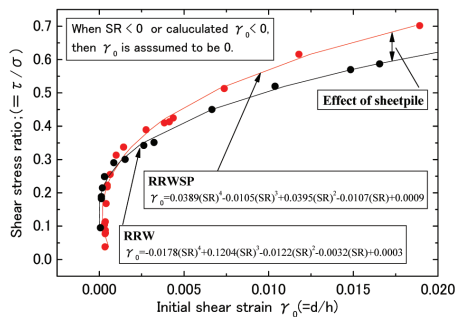


Figure 6. Initial loading curves of embedded layer (RRWSP) and sub layer (RRW).

sheetpile, with normalization by the thickness of the embedded layer.

The shear stress ratio was evaluated based on the measured response acceleration of the reinforced backfill, while considering the earth pressure exerted from the unreinforced backfill. The earth pressure was estimated using the original Mononobe-Okabe method, where the peak angle of internal friction of the unreinforced backfill was set equal to 51 degrees, based on the relevant plane strain compression test results (Koseki et al., 2004). The modified Mononobe Okabe method (Koseki et al., 1998) was also applied to evaluate the earth pressure after the formation of the failure plane in the unreinforced backfill.

The shear strain increments of each subsoil layer during seismic excitation was separated into two components; one is initial shear strain which is mobilized due to the initial loading effect during the shaking; the other is cumulative strain due to cyclic loading effect.

The relationships between the shear stress ratio and the sum of initial shear strain γ_0 induced by the first loading effect in each layer are shown in Fig. 6. The measured data were approximated by polynomial equations which are also shown in Fig. 6. It will be referred as “initial loading curve” herein.

The effect of the sheetpile in reducing the sliding displacement was evaluated by comparing two initial loading curves for embedded layer and sub layer

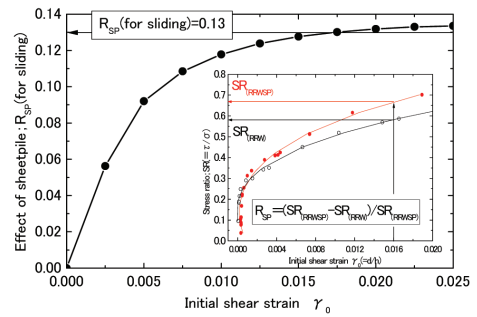


Figure 7. Effect of sheetpile for sliding in embedded layer.

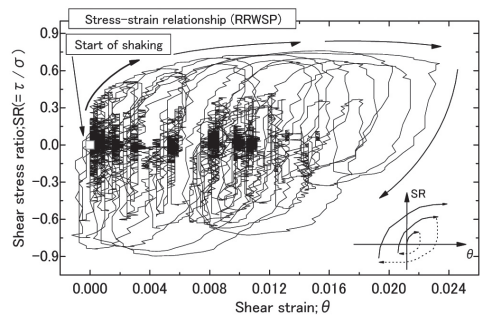


Figure 8. Stress-strain relationship of reinforced backfill behind the wall facing with sheetpile.

(Fig. 6). The ratio R_{SP} , as defined in Fig. 7, was converged into 0.13, which was employed during all the shaking steps in the computation. It is assumed herein that the sheetpile would share some amount of SR by a ratio of R_{SP} (for sliding).

In addition to the initial shear strain, the cumulative strain which was induced by cyclic loading effect was also considered. The cumulative damage concept (Tatsuoka et al., 1982) was applied to evaluate the cumulative strain. In evaluating this component, the effect of the sheetpile wasn't taken into account because the amount of cyclic loading effect was found to be negligibly smaller than the initial loading effect in the analyzed case.

3.3 Shear deformation of reinforced backfill

In a similar manner to the above, relationships between the shear stress ratio and the shear strain mobilized in the reinforced backfill were evaluated as shown in Fig. 8. The shear strain of reinforced backfill was also divided into two components: the initial shear strain and the cumulative strain.

The initial loading curves for the reinforced backfill behind the facing with embedded sheetpile (RRWSP) and without sheetpile (RRW) are shown in Fig. 9. The effect of the sheetpile was evaluated by comparing two initial loading curves. As shown in Fig. 10, the

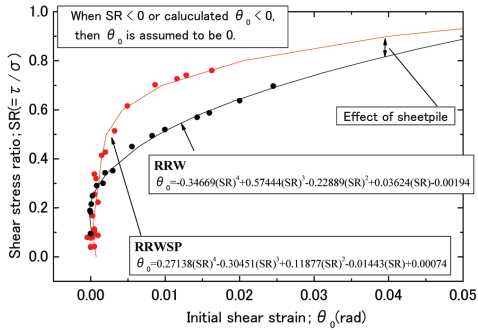


Figure 9. Initial loading curve of reinforced backfill with embedded sheetpile (RRWSP) and without sheetpile (RRW).

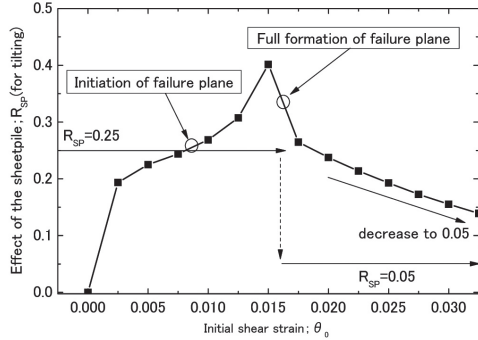


Figure 10. Effect of sheetpile for tilting.

ratio R_{SP} (for tilting) changed during the formation of the failure plane in the unreinforced backfill. For simplicity, R_{SP} (for tilting) before full formation of failure plane in unreinforced backfill was set equal to 0.25 in the computation, after which it was decreased to 0.05.

3.4 Comparison between the computation and test results

The computed and measured displacements of the wall facing are plotted versus the base acceleration in Fig. 11. Computed base sliding before full formation of failure plane agreed reasonably with the measured ones. This is because the above modeling was made based on the same test results.

The formation of the failure plane in unreinforced backfill was evaluated by the amount of shear strain in the affected region which was calculated from the computed displacements of wall facing and the observed angle of failure plane. The threshold value of shear strain in the unreinforced backfill was set equal to 10%, which corresponded to the residual state in relevant plane strain compression test results. Full formation of failure plane was well predicted by the above assumption.

To compute base sliding after full formation of failure plane, Newmark's sliding block method was

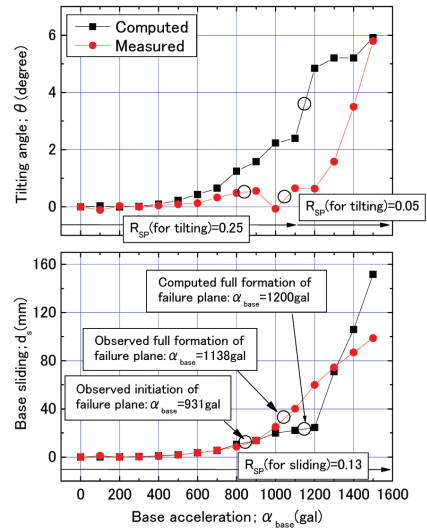


Figure 11. Computed displacements of wall facing.

applied, where the threshold acceleration was set equal to 500 gals based on the analysis using the two wedge method with the residual angle of internal friction set equal to 43 degree, while considering the friction resistance of the embedded layer acted on the sheetpile.

Computed tilting angle was over-estimated in general. This is because the effect of the sheetpile for tilting was under-estimated especially after the formation of the failure plane (Fig. 10).

4 CONCLUSIONS

Based on the 1-g shaking table model test results, effect of the embedded sheetpile was studied. The formerly developed procedure to predict the wall displacements was modified to introduce the observed effect of the sheetpile. Computed displacements using the modified procedure agreed well with measured ones. Further studies on the effects of the embedded length and thickness of the sheetpile are required to apply this method to the actual design.

REFERENCES

- Koseki, J., Tatsuoka, F., Munuf, Y., Tateyama, M. and Kojima, K. (2004). "Evaluation of seismic displacement of reinforced walls", Proc. of 3rd Asian regional conference on Geosynthetics, Seoul, pp. 217-224.
- Watanabe, K., Munuf, Y., Koseki, J., Tateyama, M. and Kojima, K. (2003). "Behaviors of several types of retaining walls subjected to irregular excitation", Soils and Foundations, Vol. 43(5), pp. 13-27.
- Tatsuoka, F. and Silver, M.L. (1982). "Undrained Stress-strain behaviour of sand under irregular loading", Soils and Foundations, Vol. 21 (1), pp. 52-65.